Layered structure transformations and exfoliation of h-BN during thermal cycling

Zhengyu Yan[1], Amor Abdelkader[2], Wajira Mirihanage[1, *]

[1]Depertment of Materials, The University of Manchester, Manchester M13 9PL, UK

[2] Faculty of Science and Technology, Bournemouth University, Poole BH12 5BB, UK.

*corresponding author: wajira.mirihanage@manchester.ac.uk

Abstract

Understanding structural transformation of hexagonal boron nitride (h-BN) at elevated temperatures is critical to obtain 2D-h-BN through thermal exfoliation. Therefore, in-situ X-ray diffraction data is collected from h-BN powders while subjecting them to a thermal cycle. The potential to define the structure order during temperature variations is revealed by using an index (I_{3D}). It was revealed that no direct correlation with the degree of exfoliation of layered structure and the structural order change during thermal cycling. Furthermore, particle size dependence of the structure order under elevated temperature is also mapped.

KEYWORDS: 2D materials, synchrotron X-ray powder diffraction, structure order

Bulk Hexagonal boron nitride (h-BN) has a similar layered hexagonal structure as graphite and potential to produce two-dimensional h-BN through exfoliation [1]. Compared to graphite, h-BN consists of the hexagon stacking directly on each other with alternatively placed B and N atoms [2]. To produce graphene-like 2D atomically thin h-BN, thermal exfoliation in the air has been suggested as a potential technique that can be extended to large scale production [3]. X-ray diffraction (XRD) studies have been employed to study the evolution of the crystalline lattice of h-BN under varying temperatures [4]–[7]. However, detailing the intermediate structural states during thermal treatments remains unclear.

To overcome ambiguities associated with lattice structural distortions during thermal treatment and provide quantified representations, 'graphitisation index' is proposed by Thomas et al. [7], which is generalised and named as 3D Index (I_{3D}) here, can be written as;

$$I_{3D}. = [\ \sum I\,(1\,0\,0) + \sum I\,(1\,0\,1)\ ]/\ \sum I\,(1\,0\,2) \qquad \#(1)$$

where $\sum I(hkl)$ refers to the integrated intensity of a given XRD peak with the indexes of *h*, *k,* and *l*. One constraint is that I_{3D} can only be applied to h-BN, graphene, or similar material when (102) peak appears, which is associated with the high ordered structure. Thomas et al. [7] showed the index (referred as I_{3D} here) of 1.60 for fully graphitised BN_g and suggested that the value increases with the decreasing structural order. The I_{3D} value could hence reach an upper range of 40-50, at which point the area of the (102) peak becomes about to disapear. The emphasis on (102) peak was because of its better sensitivity towards the order degree change than the (103) or (004) peaks, and negligible influence by the orientation effects. However, the particle size effect and recovery process was not considered in the study [7].

In general, I_{3D} can be regarded as a parameter that describes the structural order [8], [9]. Thus, in this contribution, I_{3D} is employed to provide a preliminary intuitive description of the structural transformation of h-BN at elevated temperatures.

In situ thermal exfoliation experiments were conducted in beamline I11, Diamond Light Source (UK), as schematically shown in Figure 1. Groups of 1 μm, 9 μm and 15 μm nominal particle size samples were separately subjected to in situ XRD measurements during heating and cooling. The h-BN powders were commercially sourced (the true particle size distribution is characterised by Bettersize Instrument, BT-9300ST as shown in supplementary material Fig. S1). The h-BN experimental samples were prepared by compacting the powder into 10 mm diameter disks with 2 mm thickness. The powder disk was placed within the customized electrical resistance furnace to carry out the heating and cooling cycles. During the heating processes, samples were heated up to 1263 K with rate of 4 K/min and kept for 60 mins in the air, then cooled down to room temperature (approximate cooling rate stay around 5 K/ min). The powder samples diffracted the incident X-ray beam of 25 keV, and a two-dimensional Pixima detector, which was placed 1500 mm away from the sample position, was used to record the XRD signals. The partially exfoliated powder is obtained after the thermal treatment. Extended experimental details can be found in ref. [4].
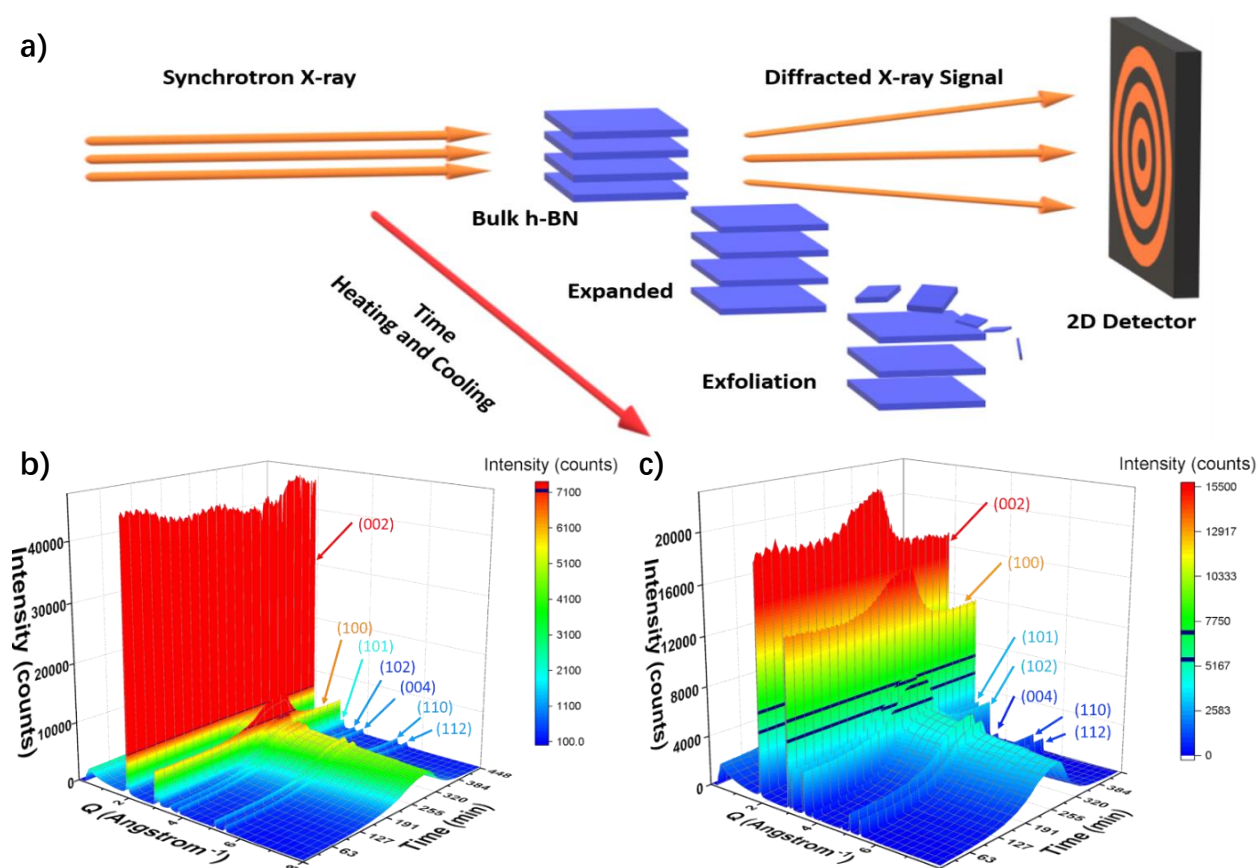

Figure 1 a) Experimental set up of h-BN thermal exfoliation; In-situ X-ray diffraction results of b) 1 μm and c) 15 μm h-BN powder samples. The x, y, z -axis are Q (Å⁻¹), time (min) and Intensity (counts) respectively. The dark lines in the middle are labelled for easier view.

Sharp diffraction peaks were observed from h-BN samples, as shown in Figure 1 b) and c), indicating

a well-ordered crystal structure at the beginning of the process. The background intensity increases with increasing temperature due to the thermal scattering. The inter-planner spacing increases linearly, apart from the (100), while the integrated peak intensities decrease. During the cooling process, the material tends to recover to its initial state. The inter-planner distances, attributed to Q, recovered but the peak intensities did not, especially for the 15 μm sample, which showed a large intensity difference. The particle size causes the diffraction profile difference between the two samples, especially seen in (100), (101) and (102). The layered structure gives a strong diffraction signal of (002).
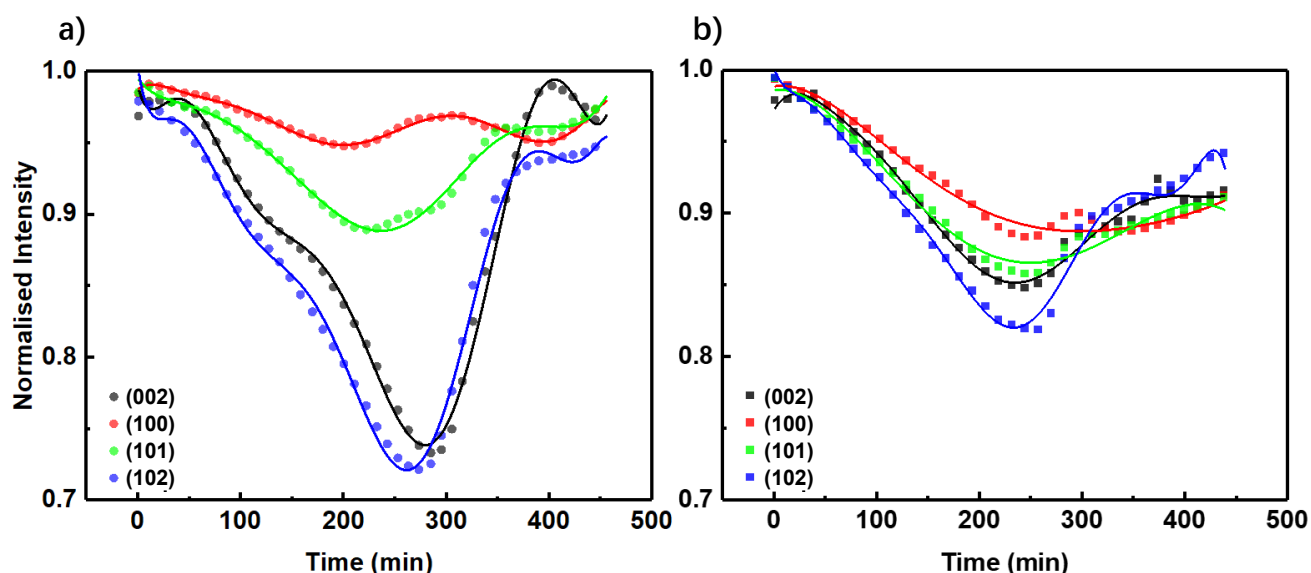

Figure 2 Normalized integrated peak intensity to maximum value versus time a) 1 μm and b) 15 μm h-BN particles: black (002), red (100), green (101), blue (102)

The integrated peak intensity (background removed) attributes for crystal structural details. As shown in Figure 2, the intensity decreases with the increasing temperature due to the thermal scattering [10]. This observation is different from the heat treatment of turbostratic BN particles that transformed to graphitic BN [5], where the intensity increased and the peak profile sharpened. In this experiment, well-ordered h-BN is used, and no phase transformation during the process. The maximum temperature was adjusted below the oxidation temperature ~1273 K [3], [11], and the material recovered to the initial state after heating and cooling. The oxidation did not appear as an influential problem as no new XRD peaks that indicate the new phases appear during the heating or cooling, as shown in Fig 1.b and c. The data were carefully examined to detect XRD peaks associated with BNO or other potential oxide phases (010) for $B(OH)_3$ [12] that may form during the experiments. Additionally, the heat treatment of h-BN under 1263 K 60 min only indicated a limited oxidation related weight gain for samples as previously reported [3]. Therefore, effects from the oxidation are reasonable to consider as negligible for the results reported in this work. As shown in Figure 2, (002) and (102) peaks indicate a greater change during the thermal cycle as the layered structure, held by Van der Waal's force, expands more easily in the c-axis direction. The (100) peak intensity shows relatively low variation, presumably due to a stronger B-N covalent bond. The 1 μm particle size sample shows more significant intensity variation in the c-axis direction than for 15 μm particle size; drop of integrated intensity of (002), 17% for 1 μm and 28% for 15 μm. However, in consideration with the a-axis direction 1 μm shows much less

variation of (100) intensity, which could be caused by the intrinsic low diffraction intensity of (100), as seen in Figure 1. This may be explained by the tendency of smaller particles stacking stronger along the c-axis, as a result the planar area of each monolayer decreases, which results in comparatively severe structure variation in c-axis direction. This means fewer defects are formed within the single layer during the heating process. Hence, the (100) is more rigid for smaller particle sizes. The 15 μm shows a similar intensity change in the range of 12% ~ 17% for all these peaks. At the end of thermal cycle, there is an intensity reduction compared to the initial state caused by the exfoliation related peeling off [4].

The I_{3D} evolution presented in Figure 3 shows that the I_{3D} increases with the increasing temperature due to the higher disorder in the crystal structure. When the exfoliation into the 2D allotrope is considered, lattice defects formed under such conditions could be a triggering to initiate the exfoliation [13], [14]. When it cools down, I_{3D} decreases to a value almost close to the initial state, even though some differences appear in individual peak intensities. This means the structure order of the bulk material (which remains) is not affected through the process. However, at the end, drop of integrated peak intensity suggests some disintegration (exfoliation) of material under invitation (Figure 2). With respect to that, constant I_{3D} indicating that the structure order, which can be evaluated through I_{3D}, is independent from the exfoliation process.
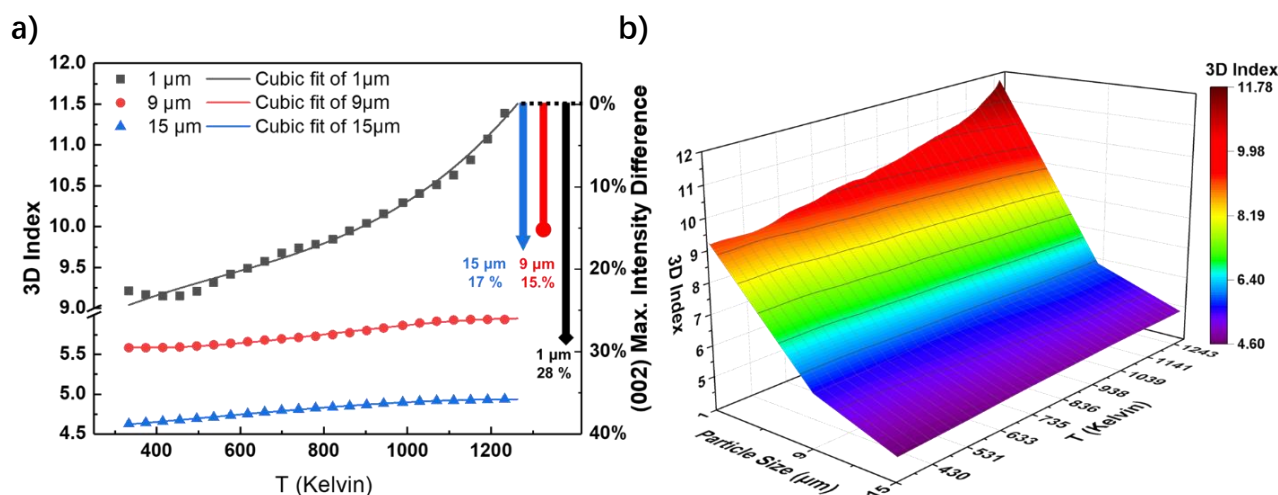

Figure 3 a) Averaged heating and cooling I_{3D} versus temperatures; the right y-axis gives the maximum integrated intensity variation value of (002) plane throughout the heat treatment experiment b) I_{3D} map with axis parameters of particle size, temperature and 3D Index

According to Figure 3 a), smaller the particle sizes introduce considerably higher I_{3D} shifting range during heating. Similar behaviour is confirmed for the (002) peak intensity variation also (Figure 2). Although the changes in the structure of smaller particles are more pronounced during heating, their exfoliation is less significant when compared to the 15 μm particles. A higher intensity difference observed for 15 μm (after cooling) explains their tendency to exfoliation. Upon heating, the low surface to volume ratio of the large particles concentrates the defects in the outer part of the grains and slows down any changing in the inner part. This inhomogeneity response to the heating creates residual stress in the large particles that promotes the exfoliation [15], [16]. The I_{3D} values for both heating and cooling processes are similar at a given temperature. The deviation to the averaged I_{3D} value is less than 2% for all the particle sizes. To demonstrate structural order considering particle size and temperature 3D map for h-BN is shown in Figure 3 b) and the

points on the curved surface gives a unique coordinate particle size, temperature, and structure order I_{3D}. This enables an intuitive approach to evaluating the structure transformation of the layered structure materials, which is consistent during heating or cooling.

In conclusion, multiple XRD peaks based analysing approach to understand the structural order of layered materials was demonstrated. The analysis based on 3D Index (I_{3D}), a ratio of different integrated Braggs peaks intensity, illustrates a quantified representation of structure order. The smaller particles tend to have greater I_{3D} value and larger structural variation upon heating. The I_{3D} value recovered to the initial level after cooling, while the integrated diffraction intensity dropped. These results proved that the exfoliation is independent of the lattice order and probably more related to the residual stresses and surface defects appear during the heating-cooling cycles. While this initial work is focused on the h-BN, and the generality of the behaviour in other layered material are proposed and examined through the demonstrated approach here.

Supplementary Material

Actual particle size distribution of nominal 1 μm , 9 μm and 15 μm samples.

Author Contributions

AA and WM conceived the approach, designed, and carried out the experiments. ZY analysed the data and drafted the manuscript with inputs from WM and AA

References

[1] Z. Wang, Z. Tang, Q. Xue *et al.*, 'Fabrication of Boron Nitride Nanosheets by Exfoliation', *The Chemical Record*, vol. 16, no. 3, pp. 1204–1215, Jun. 2016, doi: 10.1002/tcr.201500302.

[2] R. S. Pease, 'An X-ray study of boron nitride', *Acta Crystallographica*, vol. 5, no. 3, pp. 356–361, May 1952, doi: 10.1107/S0365110X52001064.

[3] Z. Cui, A. J. Oyer, A. J. Glover, H. C. Schniepp, and D. H. Adamson, 'Large Scale Thermal Exfoliation and Functionalization of Boron Nitride', *Small*, vol. 10, no. 12, pp. 2352–2355, Jun. 2014, doi: 10.1002/smll.201303236.

[4] Z. Yan, A. Abdelkader, S. Day, C. Tang, C. Casiraghi, and W. Mirihanage, '*In situ* probing of the thermal treatment of h-BN towards exfoliation', *Nanotechnology*, vol. 32, no. 10, p. 105704, Mar. 2021, doi: 10.1088/1361-6528/abce2e.

[5] S. Alkoy, C. Toy, T. Gönül, and A. Tekin, 'Crystallization behavior and characterization of turbostatic boron nitride', *Journal of the European Ceramic Society*, vol. 17, no. 12, pp. 1415–1422, Jan. 1997, doi:

10.1016/S0955-2219(97)00040-X.

[6] B. Abendroth, R. Gago, F. Eichhorn, and W. Möller, 'X-ray diffraction study of stress relaxation in cubic boron nitride films grown with simultaneous medium-energy ion bombardment', *Applied Physics Letters*, vol. 85, no. 24, pp. 5905–5907, Dec. 2004, doi: 10.1063/1.1836868.

[7] J. Thomas, N. E. Weston, and T. E. O'Connor, 'Turbostratic Boron Nitride, Thermal Transformation to Ordered-layer-lattice Boron Nitride', *J. Am. Chem. Soc.*, vol. 84, no. 24, pp. 4619–4622, Dec. 1962, doi: 10.1021/ja00883a001.

[8] L. Nistor, V. Teodorescu, C. Ghica, J. Van Landuyt, G. Dinca, and P. Georgeoni, 'The influence of the h-BN morphology and structure on the c-BN growth', *Diamond and Related Materials*, vol. 10, no. 3–7, pp. 1352–1356, Mar. 2001, doi: 10.1016/S0925-9635(00)00377-0.

[9] M. G. Balint and M. I. Petrescu, 'An attempt to identify the presence of polytype stacking faults in hBN powders by means of X-ray diffraction', *Diamond and Related Materials*, vol. 18, no. 9, pp. 1157–1162, Sep. 2009, doi: 10.1016/j.diamond.2009.02.035.

[10] K. Lonsdale, 'X-Ray Scattering by Thermal Vibrations in Crystals', *Nature*, vol. 162, no. 4110, pp. 216–216, Aug. 1948, doi: 10.1038/162216a0.

[11] D. Li, C. Zhang, B. Li, F. Cao, and S. Wang, 'Effects of heat treatment on properties of boron nitride fiber', *Sci. China Technol. Sci.*, vol. 55, no. 5, pp. 1376–1380, May 2012, doi: 10.1007/s11431-012-4750-8.

[12] B. Yu, W. Xing, W. Guo *et al.*, 'Thermal exfoliation of hexagonal boron nitride for effective enhancements on thermal stability, flame retardancy and smoke suppression of epoxy resin nanocomposites via sol–gel process', *J. Mater. Chem. A*, vol. 4, no. 19, pp. 7330–7340, 2016, doi: 10.1039/C6TA01565D.

[13] Z.-L. Hou, M.-S. Cao, J. Yuan, X.-Y. Fang, and X.-L. Shi, 'High-temperature conductance loss dominated defect level in h-BN: Experiments and first principles calculations', *Journal of Applied Physics*, vol. 105, no. 7, p. 076103, Apr. 2009, doi: 10.1063/1.3086388.

[14] Z. Li, R. J. Young, C. Backes *et al.*, 'Mechanisms of Liquid-Phase Exfoliation for the Production of Graphene', *ACS Nano*, p. acsnano.0c03916, Jul. 2020, doi: 10.1021/acsnano.0c03916.

[15] M. S. Omar and H. T. Taha, 'Lattice dislocation in Si nanowires', *Physica B: Condensed Matter*, vol. 404, no. 23–24, pp. 5203–5206, Dec. 2009, doi: 10.1016/j.physb.2009.08.304.

[16] C. Q. Sun, 'Size dependence of nanostructures: Impact of bond order deficiency', *Progress in Solid State Chemistry*, vol. 35, no. 1, pp. 1–159, Jan. 2007, doi: 10.1016/j.progsolidstchem.2006.03.001.
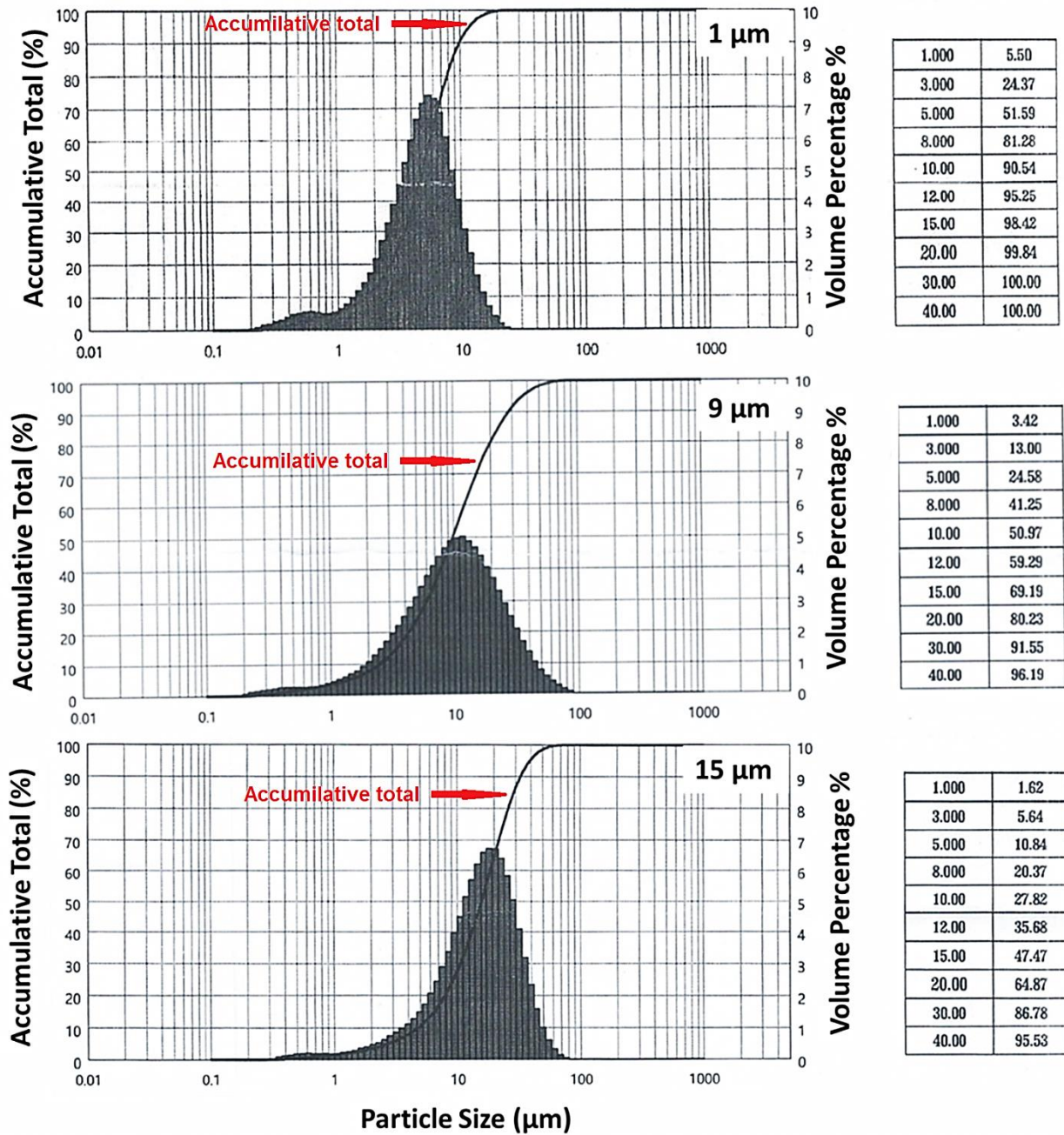
Figure S1: h-BN particle size distribution of 1 µm, 9 µm and 15 µm characterised by Bettersize Instrument, BT-9300T. The D10, D50 and D90: 1 µm sample(1.669 µm, 4.881 µm, 9.853 µm, SPAN = 1.676), 9 µm sample (2.542 µm, 9.791 µm, 28.08 µm, SPAN = 2.617), 15 µm sample (4.690 µm, 15.66 µm, 32.74 µm, SPAN = 1.791).